Measurement report: Impact of emission control measures on environmental persistent free radicals and reactive oxygen species – A short-term case study in Beijing

Yuanyuan Qin[1], Xinghua Zhang[2], Wei Huang[3], Juanjuan Qin[1], Xiaoyu Hu[1], Yuxuan Cao[1], Tianyi Zhao[1,5],

5   Yang Zhang[1,6], Jihua Tan[1], Ziyin Zhang[4], Xinming Wang[5], Zhenzhen Wang[7]

[1]College of Resources and Environment, University of Chinese Academy of Sciences, Beijing, 100049, China

[2]Sinopec (Dalian) Research Institute of Petroleum and Petrochemicals Co., Ltd, Dalian, 116045, China

[3]Institute of Environmental Reference Materials of Environmental Development Centre of Ministry of Ecology and Environment, Beijing, 100029, China

10   [4]Institute of Urban Meteorology, China Meteorological Administration, Beijing, 100089, China

[5]Guangzhou Institute of Geochemistry, Chinese Academy of Sciences, Guangzhou, 510640, China

[6]Beijing Yanshan Earth Critical Zone National Research Station, Beijing, 101408, China

[7]School of Environmental Engineering, Changsha Environmental Protection Vocational College, Changsha, 410004, China

Correspondence to: Yang Zhang (zhangyang@ucas.ac.cn) and Jihua Tan (tanjh@ucas.ac.cn)

15

20

Abstract. A series of emission control measures implemented by the Chinese government have effectively reduced air

pollution of multiple pollutants in many regions of the country in recent decades. However, the impacts of these control

measures on environmental persistent free radicals (EPFRs) and reactive oxygen species (ROS), the two groups of chemical

species that are known to be linked with adverse human health effects, are still not clear. In this study, we investigated the

levels, patterns, and sources of EPFRs and gas- and particle-phase ROS (referred to as G-ROS and P-ROS, respectively) in

Beijing during the 2015 China Victory Day Parade period when short-term air quality control measures were imposed. The

strict control measures reduced ambient EPFRs, G-ROS, and P-ROS by 18.3%, 24.1%, and 46.9%, respectively. EPFRs in the

non-control period (NCP) tended to be radicals centered on a mixture of carbon and oxygen, while those in the control period

(CP) were mainly oxygen-centered free radicals. The contribution of G-ROS to the atmospheric oxidizing capacity increased

and/or that of P-ROS decreased during CP compared to NCP. The "Parade Blue" days were largely attributed to the dramatic

reduction in secondary aerosols, which were also largely responsible for EPFRs and ROS reductions. Our findings demonstrate

how effective control measures are in reducing EPFRs and ROS and provide insights into the correlations, sources, and

formation processes of EPFRs and ROS.
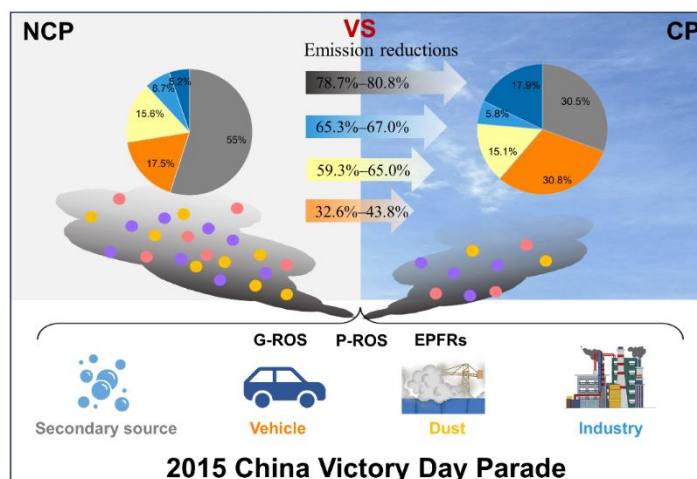
Graphical abstract

1 Introduction

Free radicals are atoms or molecules that contain at least one unpaired electron, which enables free radicals highly reactive (Khan et al., 2018). Free radicals attached to particles with a lifetime of several days or longer are defined as environmental persistent free radicals (EPFRs, e.g., phenoxy and semiquinone free radicals), to distinguish from traditional free radicals with a shorter lifetime (Li et al., 2022). The excessive lifetime of EPFRs will lead to a higher risk of human exposure to this group of chemical pollutants (Vejerano et al., 2018). It was estimated that human exposure to EPFRs in Beijing is equivalent to approximately 33 cigarettes tar EPFRs inhaled per day (Xu et al., 2020). Numerous toxicological studies have shown that inhalation of EPFRs is linked to a variety of diseases, such as chronic lung disease and respiratory dysfunction, and thus has detrimental effects on human health (Chen et al., 2019b; Thevenot et al., 2013; Vejerano et al., 2018).

Previous studies have shown that the concentration of EPFRs in atmospheric particles varied from 1.60×10^{13} spins/m^3 to 8.97×10^{15} spins/m^3 (Wang et al., 2022; Li et al., 2022). EPFRs are primarily derived from combustion sources such as vehicle exhaust and biomass burning (Wang et al., 2019b), and can also result from dust and secondary processes in the atmosphere. For example, EPFRs can be formed and stabilized on the surface of particulate matter containing transition metals and substituted aromatic structures emitted during combustion processes (Odinga et al., 2020; Chen et al., 2019a). Chen et al. (2018) found that dust storms can significantly increase the concentration of EPFRs in $PM_{2.5}$. In addition, EPFRs can be formed from polycyclic aromatic hydrocarbons (PAHs) after photolysis (Li et al., 2022). Notably, EPFRs have received widespread attention in recent years because of their ability to convert O_2 molecules into reactive oxygen species (ROS) (Chen et al., 2018). However, the sources and formation processes of EPFRs and ROS and the relationship between these two groups of pollutants are poorly understood, resulting in larger uncertainties in environmental risks assessments.

ROS are oxygen molecules that contain at least one unpaired electron, including singlet oxygen, superoxide radicals ($O_2^{\bullet-}$), OH radicals ($OH^{\bullet}$), hydrogen peroxide (H_2O_2), as well as organic radicals (Tong et al., 2018; Arangio et al., 2016). ROS have been found in wood combustion (Zhou et al., 2018), vehicle exhaust (Verma et al., 2010), and cooking emissions (Wang et al., 2020a). ROS can also form on the surface of particles or in air through photochemical reactions and reactions with ozone (O_3) under dark conditions (Zhu et al., 2018). ROS play an active role in the atmospheric environment and determine the oxygenation of atmospheric aerosols. More importantly, ROS can cause oxidative stress, resulting in particle-related health

65 effects (Huang et al., 2018b). Oxidative stress, referred to as a state of disequilibrium between oxidizing agents (ROS) and antioxidant defense capacity, has been recognized as a major contributor to organism diseases (Fang et al., 2017). Thus, measurement and analysis of the level and sources variation of ROS are vital for understanding the mechanism of ROS formation and its effect on human health.

To mitigate air pollution and associated adverse health effects, the Chinese State Council issued a series of air quality control
70 plans since 2013, termed as the "Action plan on Prevention and Control of Air Pollution", which tremendously reduced the concentration of air pollutants in the following decade (Huang et al., 2018a; Niu et al., 2022). In addition, the Chinese government has implemented stricter short-term control measures to ensure excellent air quality during certain special periods such as when hosting mega-events (Wang et al., 2019a; Schleicher et al., 2012). In September 2015, the China Victory Day Parade was held in Beijing, and different levels of short-term emission measures were implemented in Beijing and surrounding
75 cities (Ma et al., 2020). Particle concentrations in Beijing were substantially reduced during this period, achieving the so-called "Parade Blue" (Huang et al., 2018b). Some other air pollutants have also been investigated during this control period (Zhao et al., 2017; Zheng et al., 2016). This event also provided an excellent opportunity to quantify the effectiveness of control measures on EPFRs and ROS.

In this work, we evaluated the temporal variations in the chemical compositions of $PM_{2.5}$ and gas pollutants during the
80 period when the 2015 China Victory Day Parade was held in Beijing, aiming to explore the influence of short-term air quality control measures on EPFRs, gas phase ROS (G-ROS), and particle phase ROS (P-ROS). Additionally, the sources and formation mechanisms of EPFRs, G-ROS, and P-ROS were explored using correlation analysis and positive factorization matrix (PMF) model. The findings from this study have great implications for further understanding the sources and environmental risks of these chemical species and for the development of optimal air pollution control measures.

85 **2 Methods and Materials**

2.1 Sample Collection

Sampling was conducted on the rooftop of a five-floor building at the Institute of Remote Sensing and Digital Earth, Chinese

Academy of Sciences (117.39°E, 40.01°N), which is located between the fourth and fifth ring road in northern Chaoyang District, Beijing, China and is surrounded by residential buildings and Olympic Forest Park. A total of 76 $PM_{2.5}$ samples

90   including 38 daytime (8:00–20:00) and 38 nighttime (20:00–8:00 the next day) samples were collected on prebaked quartz filters using Digital high-flow sampler (DHA-80, Digital, Switzerland) with a flow rate of 500 L/min from August 13 to September 19, 2015. The samples were wrapped in aluminum foil and then stored in a refrigerator at -20°C until analysis.

The specific sample information is shown in Table S1. The whole sampling period is divided into four sub-periods for analysis (Table S2), with period 1 (August 13–19) and period 4 (September 4–19) having no control measures implemented

95   (referred to as non-control periods, NCP), period 2 (August 20–31) having regularly control measures, and period 3 (August 1–3) having stricter control measures, and periods 2 and 3 were defined as control periods (CP).

2.2 Chemical Analyses

Organic carbon (OC) and elementary carbon (EC) in $PM_{2.5}$ were measured by a thermal/optical carbon analyzer (model RT-4, Sunset Laboratory Inc. USA). Water-soluble ions (NO_3^-, SO_4^{2-}, Cl^-, NH_4^+, Na^+, K^+, Ca^{2+}, and Mg^{2+}) were analyzed by an ion

100 chromatography analyzer (model ICS-1100, Thermo Fisher Scientific). Elements (Li, Na, Mg, Al, K, Ca, V, Mn, Fe, Co, Cu, Zn, As, Se, Rb, Cd, Pb, and Bi) in $PM_{2.5}$ were extracted by microwave digestion with 7 mL of ultrapure water, 2 mL of HNO_3, and 1 mL of H_2O_2, and the concentrations of elements were detected using inductively coupled plasma−mass spectrometry (ICP-MS). PAHs were extracted by a liquid mixture of dichloromethane and methyl alcohol and measured using gas chromatography equipped with a mass selective detector (Agilent 6890/5973 GC/MSD). Real-time SO_2, NO_2, and O_3 were

105 monitored online by an SO_2 analyzer (Model 43i, Thermo Scientific, USA), NOx analyzer (Model 42i, Thermo Scientific, USA), and ozone analyzer (Model 49i, Thermo Scientific, USA), respectively.

2.3 EPFRs Analyses

A 28×5 mm sampled filter was cut and placed in an electronic paramagnetic resonance (EPR) spectrometer (EMX plus, Bruker, Germany) to determine the concentrations of EPFRs. The measurement parameters of the EPR spectrometer were set as follows:

110 the magnetic field strength was 3300–3450 G; the scanning time was 60 s; the microwave power was 8.0 mW; and the

modulation amplitude was 2 G. The absolute spin amount and g factor were calibrated with Mg^{2+} and Cr^{3+} standards. The total spin numbers were divided by the volume of the samples, such that the concentration of EPFRs was expressed as spins/m^3. The crucial parameters for characterizing the type and abundance of EPFRs, such as the g-factor and line width ($\Delta H_{p\text{-}p}$), were extracted from the EPR spectrum. EPFRs with g-factor less than 2.003 are attributed to carbon-centered free radicals, such as cyclopentadienyl radicals, while EPFRs with g-factor of 2.004 and above are designated as oxygen-centered free radicals, such as semiquinone radicals (Zhu et al., 2019). EPFRs with g-factor in the range of 2.003–2.004 suggested the existence of complex radicals centered on a mixture of carbon and oxygen or carbon-centered radicals containing oxygen atoms, such as phenoxy radicals (Yang et al., 2017; Hu et al., 2022).

2.4. G-ROS and P-ROS Measurements

The GAC-ROS online sampling and analysis system was used to measure the concentrations of G-ROS and P-ROS. The theory and constitutions of GAC-ROS were described in detail by Huang et al. (2016). In brief, GAC-ROS consists of a sampling section, a reaction and transportation section, and a detection section. Firstly, aerosols with aerodynamic diameter larger than 2.5 μm were removed by cyclone separator, gas was collected on the water film on the surface of the continuously rotating diffusion tube of the GAC, and PM$_{2.5}$ was trapped by supersaturated water vapor at a certain temperature. Secondly, solutions containing gas and particle samples were reacted with 2′,7′-dichlorofluorescin (DCFH) in the presence of horseradish peroxidase (HRP) in two glass reactors, respectively. Finally, a fluorescence detector was used to measure the concentrations of G-ROS and P-ROS. For data accuracy, flesh DCFH and HRP were prepared, and standard curves were created at least every two days.

2.5 Source Apportionment

We used the Environmental Protection Agency (EPA) PMF 5.0 version to perform the source apportionment of PM$_{2.5}$, EPFRs, G-ROS, and P-ROS. PM$_{2.5}$, EPFRs, G-ROS, P-ROS, OC, EC, water-soluble ions (NO$_3^-$, SO$_4^{2-}$, Cl$^-$, NH$_4^+$, Na$^+$, K$^+$, Ca^{2+}, and Mg^{2+}), and elements (Na, Mg, Al, K, Ca, V, Mn, Fe, Co, Cu, Zn, As, Se, Rb, Cd, Pb, and Bi) were included in the PMF model with a total sample number of 76. The procedure for the PMF model has been described in many previous reports (Wang et

al., 2019b; Sharma et al., 2016). Missing concentration values were replaced with "-999". The component concentration was

135 changed to half of the method detection limit (MDL) when it was lower than the MDL. The calculation formula of uncertainty

is Uncertainty=K×C, where K is the analytical uncertainty and C represents the concentrations of the chemical components.

The quality of the data was evaluated according to the signal-to-noise ratio (S/N), and species with S/N ranging from 1 to 10

were categorized as "Strong", while those with S/N ranging from 0.5 to 1 were categorized as "Weak". The tracer species were

also categorized as "Strong". The degree of rotation in the model results was controlled by the FPEAK and FKEY values.

3 Results and Discussion

3.1 Temporal Variations of Air Pollution

To investigate the effectiveness of short-term air pollution control measures on pollutants concentrations during the 2015 China

Victory Day Parade, temporal variations of $PM_{2.5}$, EC, middle molar weight PAHs (MMW-PAHs, 4 ring PAHs), elements, and

gas pollutants were first examined. As shown in Figure 1, $PM_{2.5}$ concentration decreased continuously from period 1 to period

145 3 before rebounded in period 4, with average $PM_{2.5}$ concentration being ~60% lower in CP (periods 2 and 3) than NCP (periods

1 and 4). Similarly, EC, a typical marker of fossil fuel combustion (Zhang et al., 2015; Wang et al., 2020b), was also ~57.0%

lower in CP than NCP, demonstrating that provisional control measures have significantly reduced fossil fuel combustion

emissions. Additionally, a 32% lower MMW-PAHs concentration in CP than NCP implied that the control measures were also

effective in reducing emissions from diesel vehicle exhaust (Perrone et al., 2014). The concentrations of elements also

150 decreased dramatically with a 51.4% lower concentration in CP than NCP.

Regarding the gaseous pollutants, SO_2, and NO_2 decreased by 10.8%, 51.2%, and 45.5%, respectively, during CP compared

to those in the NCP. NO_2 is mainly derived from vehicle exhaust emissions, and SO_2 is mainly from the fossil fuel (e.g., coal)

combustion (Hien et al., 2014; Ma et al., 2020). Apparently, the control measures implemented during CP have effectively

reduced emissions from industrial coal combustion and vehicle exhaust. In contrast, the reduction in O_3 during the CP was

155 much less than that of NO_2, which can be explained by the reduction in the titration reaction between O_3 and NO due to the

reduced NO emission from vehicle exhaust (Guo et al., 2016; Okuda et al., 2011).

Different diurnal variations were observed between the pollutants. The average concentrations of EC and NO$_2$ were generally higher during the nighttime (1.33 μg/m^3 and 40.2 μg/m^3, respectively) than daytime (0.82 μg/m^3 and 28.4 μg/m^3, respectively) in the whole measurement period. This is especially the case during the NCP, demonstrating increased traffic emissions and/or temperature inversions occurred at nighttime (Yang et al., 2015; Wu et al., 2012). Similar diurnal variations have also been observed previously in Agra and Beijing (Pipal et al., 2014; Lin et al., 2009). O$_3$ was higher in the daytime than nighttime, indicating intensive photochemical actions. SO$_2$ concentration significantly increased in the daytime during period 4, which may be caused by the surge in industrial activities (He et al., 2017).
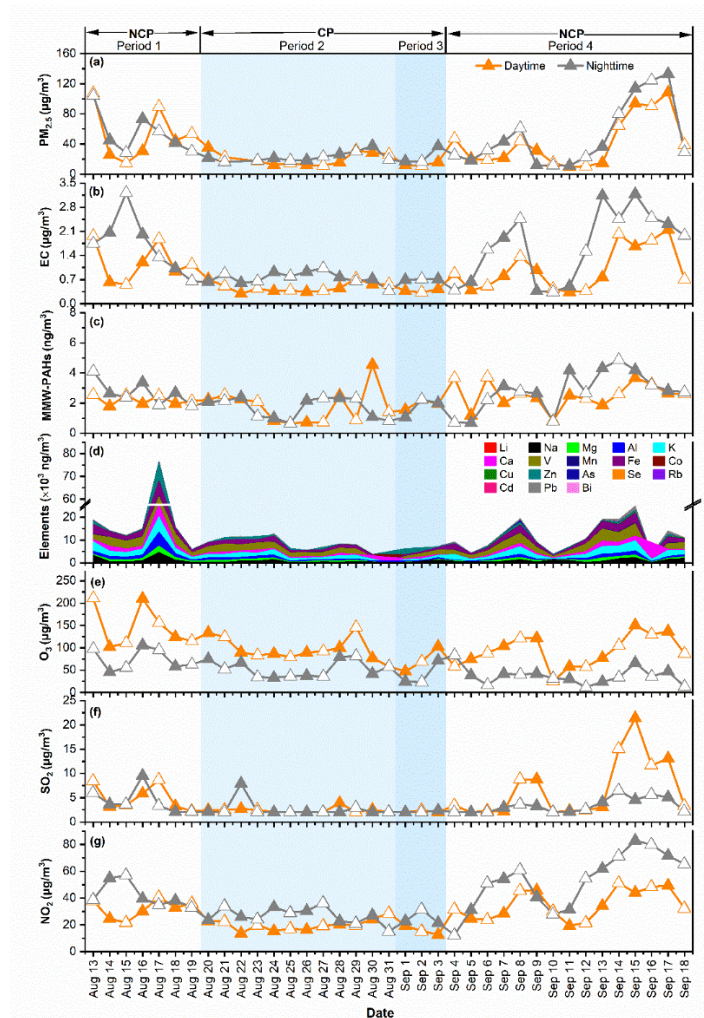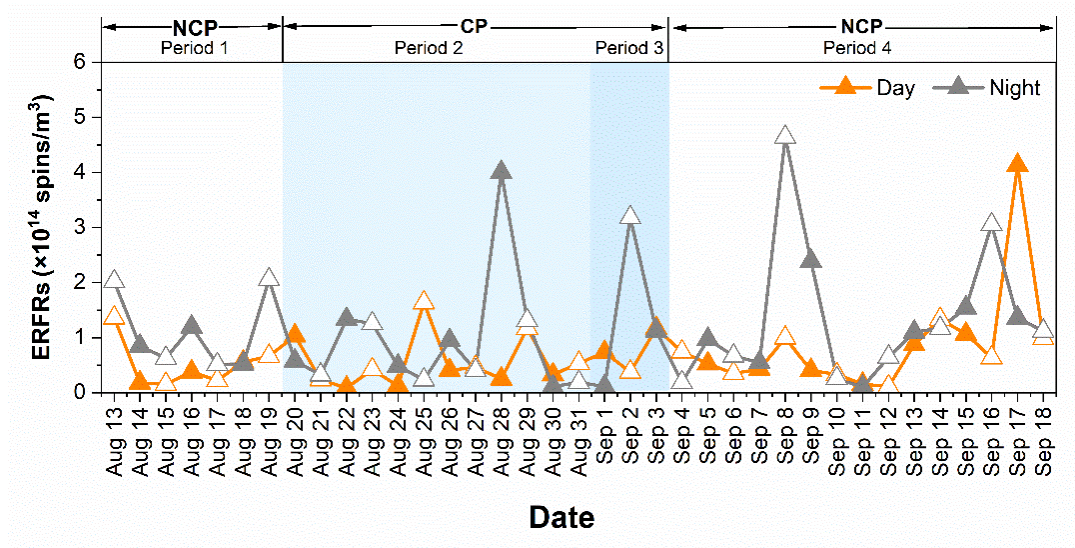

Figure 1: Temporal variations in concentrations of (a) PM$_{2.5}$, (b) EC, (c) MMW-PAHs, (d) elements, (e) O$_3$, (f) SO$_2$, and (g) NO$_2$ during the four sub-periods of the 2015 China Victory Day Parade.

3.2. Characteristics of Environmentally Persistent Free Radicals (EPFRs)

Figure 2 shows the temporal variations in EPFRs concentrations during the whole measurement period. The concentrations of

170   EPFRs in periods 1, 2, 3, and 4 were 8.07×10^{13}, 7.44×10^{13}, 1.12×10^{14} and 1.10×10^{14} spins/m^3, respectively, which represent

18.3% lower concentration during CP than NCP. The smaller percentage decrease in EPFRs than most of the other measured

pollutants (PM$_{2.5}$, EC, elements, NO$_2$, and SO$_2$) indicated that the control measures were not as effective in reducing EPFRs

concentrations due to the complex formation and transformation of EPFRs, similar to the case of O$_3$. Nevertheless, the levels

of EPFRs in PM$_{2.5}$ in this study were approximately two orders of magnitude lower than those in Beijing (1.70×10^{15}–3.50×10^{16}

175   spins/m^3) in 2016 (Yang et al., 2017) and slightly lower than those in Xi'an (1.79×10^{14} spins/m^3) in 2017 (Wang et al., 2019b),

but much higher than that in Chongqing (7.0×10^{13} spin/m) in 2017–2018 (Qian et al., 2020).

The average concentrations of EPFRs during the daytime and nighttime were 6.85×10^{13} spins/m^3 and 1.18×10^{14} spins/m^3,

respectively, indicating that nighttime samples contained more EPFRs than daylight samples, likely because the half-life times

of EPFRs were longer under dark than light conditions (Lang et al., 2022; Chen et al., 2019a). The lower EPFRs concentrations

180   during daytime may be related to the rapid conversion of EPFRs to other chemical species under strong irradiation. Besides,

increased traffic emissions during nighttime, as mentioned above, may have possibly led to higher levels of EPFRs in nighttime.

For instance, Hwang et al.(2021) found that PM$_{2.5}$ from traffic-related sources generally has higher EPFRs concentrations than

that from urban background particles.

Figure 2: Temporal variations in EPFRs concentrations during the measurement period.

The g-factor and $\Delta H_{\text{p-p}}$ values of EPFRs during the four pollution periods are depicted in Figure 3. The average g-factor was

2.00395 in NCP and 2.00429 in CP. Hence, the observed EPFRs in NCP tend to be radical centered on a mixture of carbon and

oxygen. The higher g-factor in CP, especially in period 3, suggested that oxygen-centered free radicals were attached to the

PM$_{2.5}$ samples (Li et al., 2023). It has been reported in literature that EPFRs derived from primary combustion sources (e.g.,

coal combustion and vehicle emission) generally have a lower g-factor (Chen et al., 2019c), while those from post-illumination

tend to have a greater g-factor (Chen et al., 2019a). The data presented above indicated that the generation of EPFRs with

lower g-factor was restricted during CP when the emissions from primary combustion sources were significantly reduced. It

is known that carbon-centered radicals are more unstable and easily oxidized in the atmosphere than oxygen-centered radicals

(Wang et al., 2018). Therefore, the free radicals generated during CP had stronger antioxidant properties, while those generated

during NCP were more easily oxidized. A higher level $\Delta H_{\text{p-p}}$ was observed during CP than NCP, indicating a relatively complex

path for the formation of EPFRs under strict control measure conditions. Our previous study found that secondary

photochemical reactions may lead to the production of more types of EPFRs (Zhang et al., 2022).
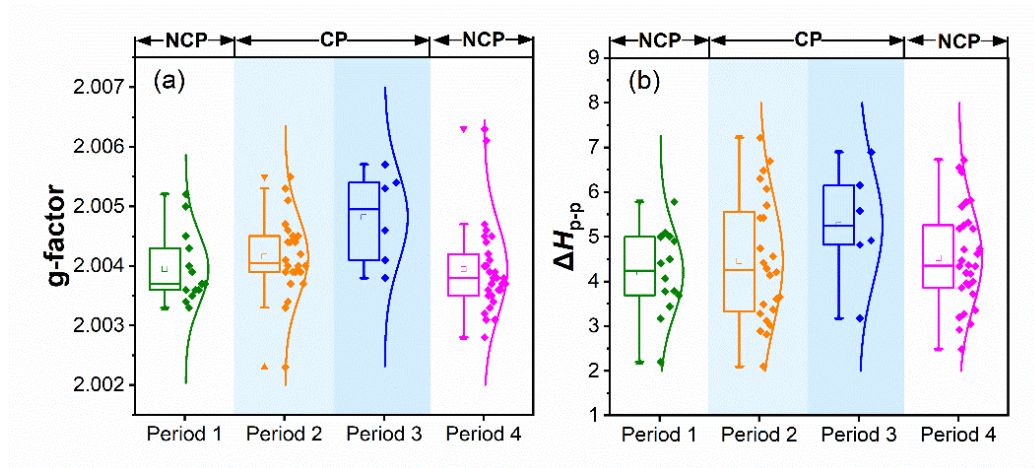
Figure 3: The (a) g-factor and (b) $\Delta H_{p\text{-}p}$ of EPFRs during the four pollution periods.

3.3. Reactive Oxygen Species (ROS) Activity

The ROS activity obtained here was expressed in nmol H_2O_2 equivalents m^{-3}. As shown in Figure 4, the average concentrations of G-ROS and P-ROS were 17.2 nmol H_2O_2/m^3 and 13.6 nmol H_2O_2/m^3, respectively, during NCP, decreased to 13.8 nmol H_2O_2/m^3 and 7.25 nmol H_2O_2/m^3 during period 2, and further decreased to 10.3 nmol H_2O_2/m^3 and 7.02 nmol H_2O_2/m^3 during period 3. The concentrations of ROS during CP were comparable to those observed in urban America (Wang et al., 2011) and rural China (Zhao et al., 2023; Huang et al., 2016). The percentage decreases in G-ROS and P-ROS concentrations during CP were much more than those in the EPFRs concentration. It is noteworthy that the impact of the control measures on G-ROS and P-ROS was different (Figure 5). The much higher ratios of G-ROS to P-ROS during CP than NCP suggested that the contribution of G-ROS to atmospheric oxidizing capacity was increased and/or that of P-ROS was decreased during this period. However, the control measures were clearly less effective in reducing G-ROS during period 2 than period 3.
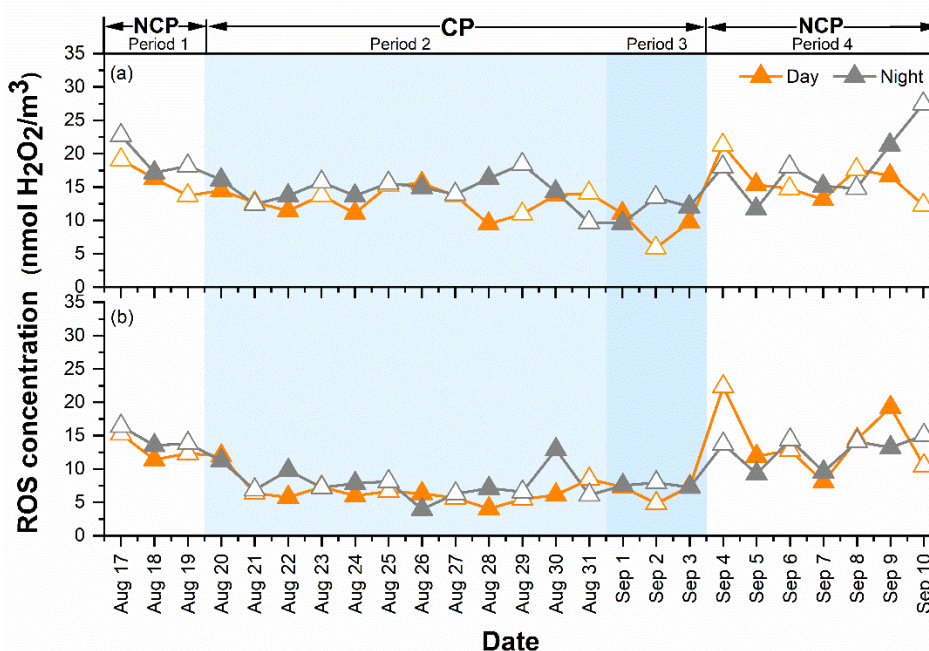
Figure 4: The concentrations of (a) G-ROS and (b) P-GOS during the whole measurement period.
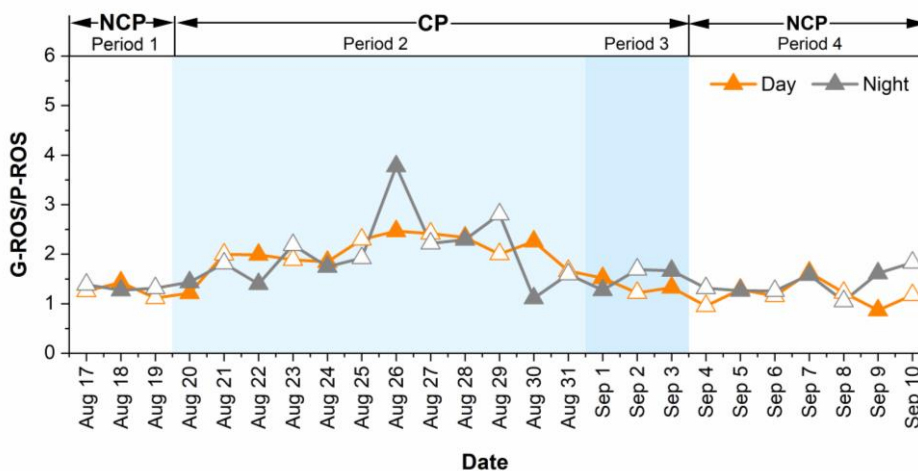

Figure 5: The ratios of G-ROS to P-ROS during the whole measurement period.

215

The average concentration of G-ROS was slightly higher at nighttime (15.8 nmol H_2O_2/m^3) than daytime (13.7 nmol H_2O_2/m^3),

so was the case of P-ROS (10.0 nmol H_2O_2/m^3 versus 9.5 nmol H_2O_2/m^3), consistent with that reported in a previous study in

Xi'an in 2021 (Ainur et al., 2023). The higher ROS levels at night are more evident from the diurnal variations shown in Figure 6. G-ROS decreased at approximately 8:00 am and then rapidly increased at 18:00 pm during all of the four sub-periods. We

220   speculated that the chemical reactions driven by NO_3 free radicals were the main source of G-ROS in nighttime in this study (Venkatachari et al., 2005). However, P-ROS decreased at approximately 3:00 am and then increased at approximately 13:00 pm. These results suggest that different formation mechanisms existed between G-ROS and P-ROS.
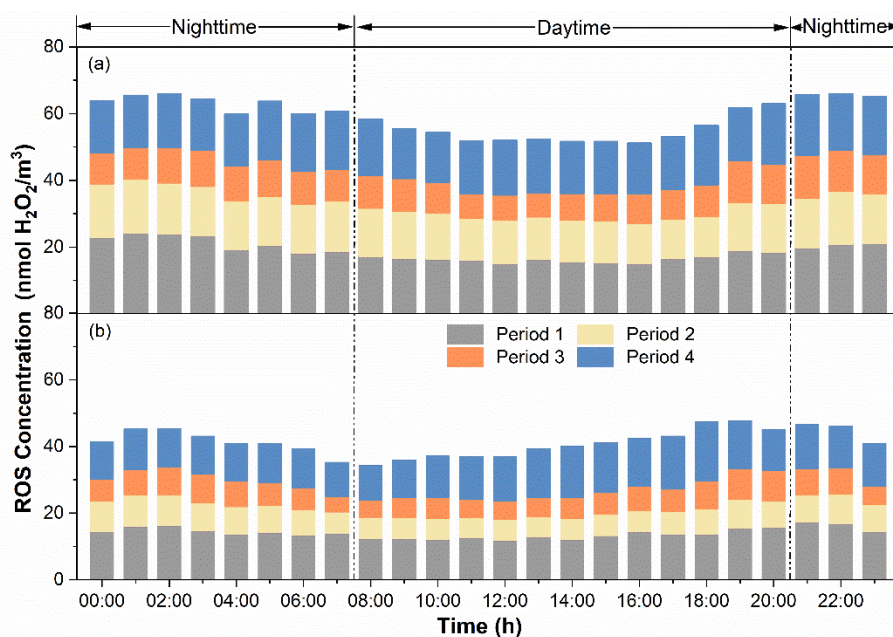

Figure 6: Diurnal variations in concentrations of (a) G-ROS and (b) P-ROS during the four pollution periods.

225   **3.4 Correlation Analysis**

Figure 7 shows the Spearman correlation of EPFRs, G-ROS, and P-ROS with other pollutants. EPFRs concentration strongly correlated with ΔH_{p-p} ($r>0.76$), indicating more abundant types of EPFRs under higher EPFR concentration condition. In addition to simple and well-defined EPFRs, such as semiquinone and cyclopentadienyl radicals, there are also many complex and unknown EPFRs in the research blind spot. AQI and $PM_{2.5}$ both positively correlated with the concentration of EPFRs

230   ($r>0.42$), suggesting that the contamination of EPFRs was significantly influenced by the relevant health index and haze. EPFRs exhibited a significant positive correlation with vehicle exhaust markers EC and NO_2 ($p<0.05$), emphasizing that vehicle exhaust emissions may be an important source of EPFRs in Beijing. Recent studies also found that EPFRs significantly

correlated with EC and NO_2 on highways, mainly related to the emissions in vehicle exhaust (Hwang et al., 2021; Li et al.,

2022). A stronger positive correlation between ERFRs and secondary inorganic ions was found in the daytime (r=0.45) than

235   nighttime (r=0.37). Meanwhile, a significant positive correlation between ERFRs and O_3 was also observed in the daytime

(p<0.1). Thus, atmospheric oxidation processes associated with EPFRs production occurred mainly during the daytime (Chen

et al., 2019b). The oxidation of different types of PAHs by O_3 could form different types of EPFRs, as demonstrated in a

previous study (Borrowman et al., 2016). Transition metals, as single-electron acceptors or shuttles (Wan et al., 2020), play a

key role not only in the formation of EPFRs but also in maintaining the long half-life of EPFRs (Pan et al., 2019; Vinayak et

240   al., 2022). Cd only significantly correlated with EPFRs in the daytime (p<0.05), while the majority of transition metals (e.g.,

Mn, Fe, V, and Cd) significantly correlated with EPFRs in the nighttime. These results suggest that EPFRs in the nighttime

were stabilized in particles via transition metals from fuel combustion processes, while an increased proportion of EPFRs was

generated via other pathways in the daytime, such as the secondary reactions mentioned above.
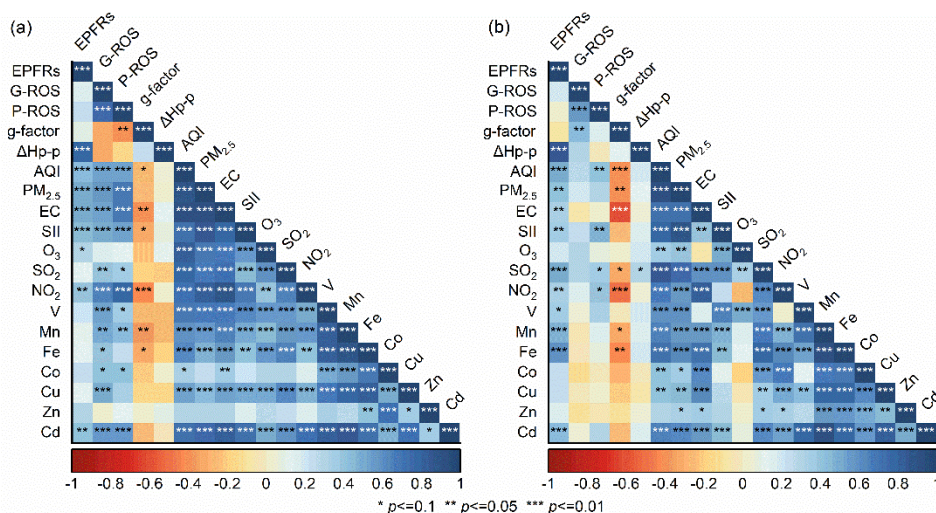

Figure 7: Spearman correlation matrix of EPFRs, G-ROS, and P-ROS concentrations with meteorological parameters, gaseous
pollutants, and $PM_{2.5}$ components during (a) daytime and (b) nighttime. SII: secondary inorganic ions. Red and blue color denote a
negative and a positive correlation, respectively.

It is not surprising that P-ROS associated with $PM_{2.5}$ more than G-ROS did. Both G-ROS and P-ROS strongly correlated with

250   EC and NO_2 (r>0.54) in the daytime, suggesting that G-ROS and P-ROS were derived from traffic-related emissions, as was

14

reported in a previous study (Stevanovic et al., 2019). G-ROS ($r>0.52$) and P-ROS ($r>0.54$) also correlated well with secondary

inorganic ions in the daytime, indicating secondary aerosols as another important source of G-ROS and P-ROS. G-ROS

significantly correlated with the majority of transition metals (e.g., V, Mn, Fe, Co, Cu, and Cd) ($p<0.1$), and P-ROS positively

correlated with metals (e.g., V, Mn, Co, and Cd), which is consistent with the current knowledge regarding the metal-induced

255   ROS formation mechanism. Transition metals have been considered to be capable of generating excess ROS such as hydroxyl

and superoxide radicals via Fenton-like reactions (Brehmer et al., 2019; Lin and Yu, 2020).

During the nighttime, there were moderate correlations between P-ROS and AQI, NO_2, SO_2, and secondary inorganic ions,

indicating the contributions of vehicle exhaust emission, coal combustion emission, and secondary formation to P-ROS. The

very weak correlation of both G-ROS and P-ROS with O_3 implied limited formation of G-ROS and P-ROS from secondary

260   reaction processes caused by O_3 in Beijing. The correlations of G-ROS and P-ROS with EPFRs were also very weak. Although

EPFRs can induce the formation of single ROS species (e.g., OH· and O_2·⁻) (Hwang et al., 2021; Guo et al., 2020), individual

ROS species is incapable of existing alone in the air, leading to different interactions between EPFRs and different ROS species.

3.5 Source Apportionment

The source profiles of $PM_{2.5}$ were analyzed using the PMF model. As shown in Figure 8, if considering the whole campaign

265   together, five major source factors were identified, including secondary aerosols, which accounted for the largest faction

(52.0%), followed by vehicle emissions (20.8%), dust sources (13.5%), industrial emissions (6.3%), and other sources (7.4%),

the total of which resolved 95.4% of $PM_{2.5}$. The percentage contributions from each source factor to $PM_{2.5}$ differed to some

extent between NCP and CP (Figure 9). For example, the percentage contributions from the above five source factors were

55.0%, 17.5%, 15.6%, 6.70%, and 5.22%, respectively, during NCP (Figure S1), and were 30.5%, 30.8%, 15.1%, 5.77%, and

270   17.9%, respectively, during CP. The large decrease in percentage contribution form secondary aerosols during CP was due to

the tremendous reductions in precursor gases (e.g., SO_2 and NO_2) of secondary aerosols. The percentage contribution from

vehicle emissions actually increased because the concentration decrease from this sector was smaller than those from the other

major source sectors (especially the factor of secondary aerosols, as discussed below).

The concentrations of $PM_{2.5}$ fractions from most source factors decreased during CP compared to NCP (Figure S2), e.g., by

15

275 78.7%, 32.6%, 63.0%, and 67.0%, from secondary aerosols, vehicle emissions, dust sources, and industrial emissions, respectively, due to the strict emission control measures implemented during CP. Thus, the achievement of "Parade Blue" days was largely attributed to the dramatic decreases in secondary aerosols, dust, and industrial emissions, a phenomenon that is consistent with that observed in a previous study during the Asia-Pacific Economic Cooperation conference reported by Sun et al. (2016). Obviously, the strict control measures during the parade period worked effectively in reducing both primary and

280 secondary pollutants.

The predominant sources of EPFRs during NCP were also secondary aerosols (50.6%), followed by vehicle emissions (33.5%), other sources (9.89%), dust sources (4.12%), and industrial emissions (1.85%). The percentage contributions of these source sectors to EPFRs during CP changed to 20.8%, 43.7%, 3.0%, 1.27%, and 31.2%, respectively. Vehicle emissions surpassed secondary aerosols to become the largest sources of EPFRs during CP. During NCP, secondary aerosols were also

285 the largest source (45.9%) of G-ROS, followed by vehicle emissions (36.6%), dust sources (11.2%), other sources (5.78%), and industrial emissions (0.54%), respectively. During CP, the contribution of secondary aerosols decreased remarkably to 18.3%, while that of vehicle emissions increased significantly to 43.0%. Similarly, the predominant source of P-ROS during NCP was also secondary aerosols (44.2%), followed by vehicle emissions (30.0%), dust sources (12.9%), other sources (10.0%), and industrial emissions (2.73%). During CP, the contribution of secondary aerosols (17.7%) to P-ROS dropped

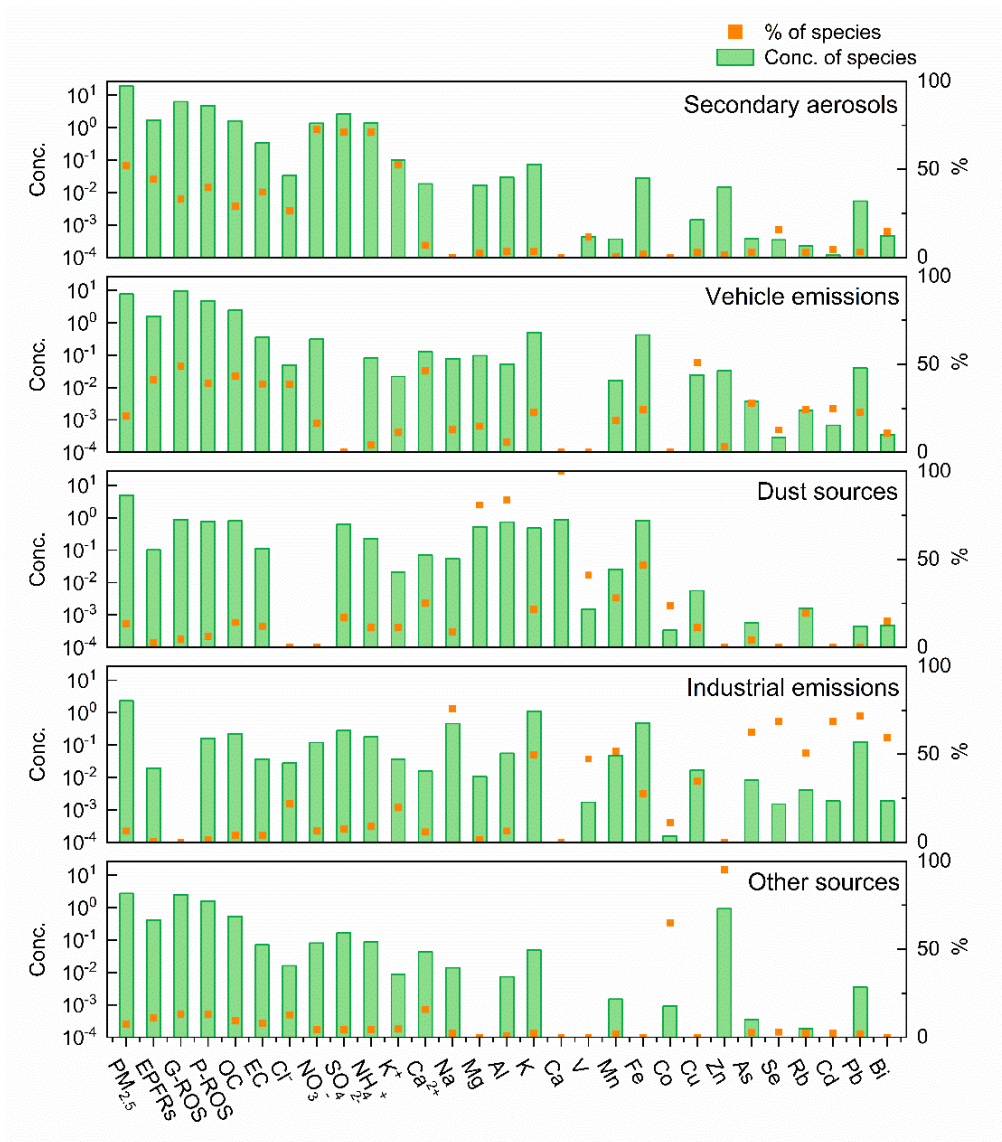290 significantly while that of vehicle emissions increased slightly to 35.2%.
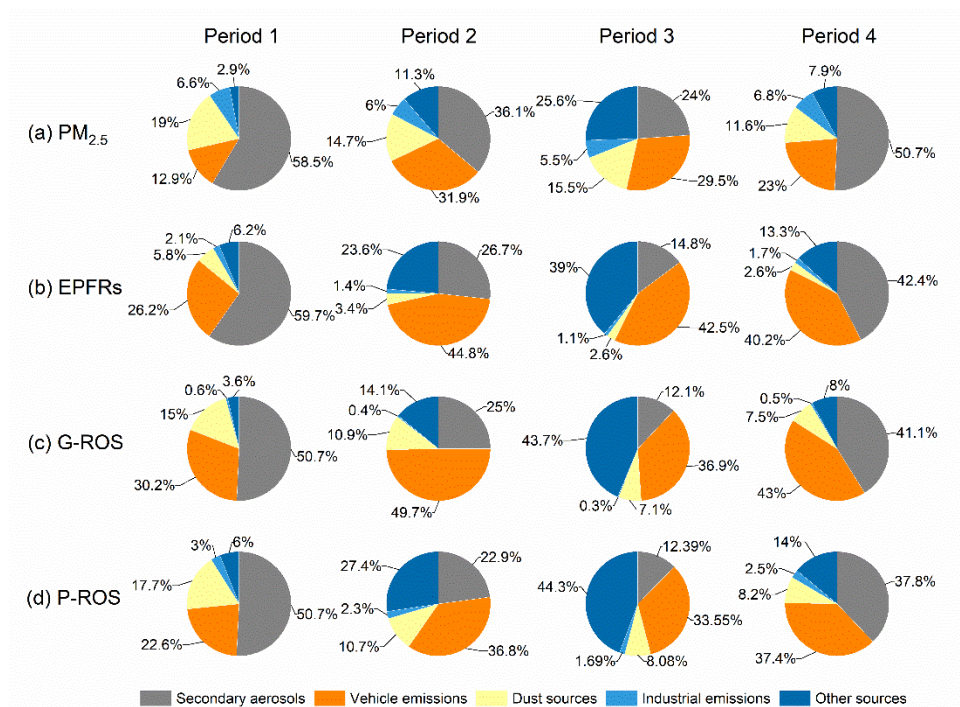
Figure 8: Profiles of different source factors of PM$_{2.5}$, including EPFRs, G-ROS, and P-ROS.

Figure 9: The contributions of different sources to PM$_{2.5}$, EPFRs, G-ROS, and P-ROS during the four sub-period.

4 Conclusions

The short-term air quality control measures on hazardous substances during the 2015 China Victory Day Parade in Beijing reduced the concentrations of EPFRs by 18.3%, G-ROS by 24.1%, and P-ROS by 46.9% during CP compared to NCP. The decrease in EPFRs was smaller than that for most other measured pollutants (e.g., PM$_{2.5}$, EC, elements, NO$_2$, and SO$_2$). The sources of EPFRs and ROS differed between day- and nighttime. EPFRs were mainly from vehicle exhaust emissions and atmospheric oxidation processes in the daytime and vehicle exhaust emissions and fossil fuel combustion in the nighttime. Vehicle exhaust, secondary aerosols, and metals from fuel combustion processes were important sources of G-ROS and P-ROS in the daytime, while vehicle exhaust and coal combustion emissions were the major contributors of P-ROS in the nighttime. The predominant sources of PM$_{2.5}$, EPFRs, G-ROS, and P-ROS during NCP were secondary aerosols, followed by vehicle emissions, but vehicle emissions surpassed secondary aerosols to become the predominant source of these chemical species during CP. The control measures implemented during CP reduced source-sector based concentrations of PM$_{2.5}$, EPFRs,

G-ROS, and P-ROS by 78.7%–80.8% from secondary aerosols, 59.3%–65.0% from dust sources, 65.3%–67.0% from industrial emissions, and 32.6%–43.8% from vehicle emissions, compared to the cases during NCP. Results from this study will benefit the development of future air quality management policies targeting EPFRs and ROS. Further in-depth studies are still needed to gain a complete understanding of the formation pathways of EPFRs and ROS under different environmental conditions.

Data availability. The data used in this study are available on the Zenodo data repository platform: https://doi.org/10.5281/zenodo.10136894 (Qin et al., 2023).

Author contribution. YZ and JT: Conceptualization and Writing – review & editing. YQ: Writing - Original Draft and Writing - Review & Editing. XZ: Writing - Review & Editing. WH: Investigation. JQ: Methodology. XH: Software. TZ: Software. ZZ: Investigation. XW: Methodology. ZW: Funding acquisition.

Competing interests. The authors declare that they have no conflict of interest.

Disclaimer. Publisher's note: Copernicus Publications remains neutral with regard to jurisdictional claims in published maps and institutional affiliations.

References

Ainur, D., Chen, Q., Sha, T., Zarak, M., Dong, Z., Guo, W., Zhang, Z., Dina, K., and An, T.: Outdoor health risk of atmospheric particulate matter at night in Xi'an, northwestern China, Environ.. Sci.. Technol., 57, 9252–9265, http://dx.doi.org/10.1021/acs.est.3c02670, 2023.

Arangio, A. M., Tong, H., Socorro, J., Pöschl, U., and Shiraiwa, M.: Quantification of environmentally persistent free radicals and reactive oxygen species in atmospheric aerosol particles, Atmos. Chem. Phys., 16, 13105–13119, http://dx.doi.org/10.5194/acp-16-13105-2016, 2016.

Borrowman, C. K., Zhou, S., Burrow, T. E., and Abbatt, J. P.: Formation of environmentally persistent free radicals from the heterogeneous reaction of ozone and polycyclic aromatic compounds, Phys. Chem. Chem. Phys, 18, 205–212,

http://dx.doi.org/10.1039/C5CP05606C, 2016.

335   Brehmer, C., Lai, A., Clark, S., Shan, M., Ni, K., Ezzati, M., Yang, X., Baumgartner, J., Schauer, J. J., and Carter, E.: The oxidative potential of personal and household $PM_{2.5}$ in a rural setting in southwestern China, Environ.. Sci.. Technol., 53, 2788–2798, http://dx.doi.org/10.1021/acs.est.8b05120, 2019.

Chen, Q., Sun, H., Wang, M., Wang, Y., Zhang, L., and Han, Y.: Environmentally persistent free radical (EPFR) formation by visible-light illumination of the organic matter in atmospheric particles, Environ.. Sci.. Technol., 53, 10053–10061,
340   http://dx.doi.org/10.1021/acs.est.9b02327, 2019a.

Chen, Q., Sun, H., Mu, Z., Wang, Y., Li, Y., Zhang, L., Wang, M., and Zhang, Z.: Characteristics of environmentally persistent free radicals in $PM_{2.5}$: Concentrations, species and sources in Xi'an, Northwestern China, Environ. Pollut., 247, 18–26, http://dx.doi.org/10.1016/j.envpol.2019.01.015, 2019b.

Chen, Q., Sun, H., Wang, J., Shan, M., Yang, X., Deng, M., Wang, Y., and Zhang, L.: Long-life type — The dominant fraction
345   of EPFRs in combustion sources and ambient fine particles in Xi'an, Atmospheric Environ., 219, 117059, http://dx.doi.org/10.1016/j.atmosenv.2019.117059, 2019c.

Chen, Q., Wang, M., Sun, H., Wang, X., Wang, Y., Li, Y., Zhang, L., and Mu, Z.: Enhanced health risks from exposure to environmentally persistent free radicals and the oxidative stress of $PM_{2.5}$ from Asian dust storms in Erenhot, Zhangbei and Jinan, China, Environ Int, 121, 260–268, http://dx.doi.org/10.1016/j.envint.2018.09.012, 2018.

350   Fang, T., Guo, H., Zeng, L., Verma, V., Nenes, A., and Weber, R. J.: Highly acidic ambient particles, soluble metals, and oxidative potential: A link between sulfate and aerosol toxicity, Environ.. Sci.. Technol., 51, 2611–2620, http://dx.doi.org/10.1021/acs.est.6b06151, 2017.

Guo, J., He, J., Liu, H., Miao, Y., Liu, H., and Zhai, P.: Impact of various emission control schemes on air quality using WRF-Chem during APEC China 2014, Atmospheric Environ., 140, 311–319, http://dx.doi.org/10.1016/j.atmosenv.2016.05.046,
355   2016.

Guo, X., Zhang, N., Hu, X., Huang, Y., Ding, Z., Chen, Y., and Lian, H.: Characteristics and potential inhalation exposure risks of $PM_{2.5}$–bound environmental persistent free radicals in Nanjing, a mega–city in China, Atmospheric Environ., 224, 117355, http://dx.doi.org/10.1016/j.atmosenv.2020.117355, 2020.

He, Z., Shi, X., Wang, X., and Xu, Y.: Urbanisation and the geographic concentration of industrial SO_2 emissions in China,
360   Urban Studies, 54, 3579–3596, http://dx.doi.org/10.1177/004209801666991, 2017.

Hien, P., Hangartner, M., Fabian, S., and Tan, P.: Concentrations of NO_2, SO_2, and benzene across Hanoi measured by passive diffusion samplers, Atmospheric Environ., 88, 66–73, http://dx.doi.org/10.1016/j.atmosenv.2014.01.036, 2014.

Hu, Y., Zhang, B., Guo, Q., Wang, S., and Lu, S.: Characterization into environmentally persistent free radicals formed in incineration fly ash and pyrolysis biochar of sewage sludge and biomass, J. Clean. Prod., 373, 133666,
365   http://dx.doi.org/10.1016/j.jclepro.2022.133666, 2022.

Huang, J., Pan, X., Guo, X., and Li, G.: Health impact of China's air pollution prevention and control action plan: An analysis of national air quality monitoring and mortality data, Lancet Planet. Health, 2, e313–e323, http://dx.doi.org/10.1016/S2542-5196(18)30141-4, 2018a.

Huang, W., Zhang, Y., Zhang, Y., Zeng, L., Dong, H., Huo, P., Fang, D., and Schauer, J. J.: Development of an automated
370   sampling-analysis system for simultaneous measurement of reactive oxygen species (ROS) in gas and particle phases: GAC-

ROS, Atmospheric Environ., 134, 18–26, http://dx.doi.org/10.1016/j.atmosenv.2016.03.038, 2016.

Huang, W., Fang, D., Shang, J., Li, Z., Zhang, Y., Huo, P., Liu, Z., Schauer, J. J., and Zhang, Y.: Relative impact of short-term emissions controls on gas and particle-phase oxidative potential during the 2015 China Victory Day Parade in Beijing, China, Atmospheric Environ., 183, 49–56, http://dx.doi.org/10.1016/j.atmosenv.2018.03.046, 2018b.

375 Hwang, B., Fang, T., Pham, R., Wei, J., Gronstal, S., Lopez, B., Frederickson, C., Galeazzo, T., Wang, X., and Jung, H.: Environmentally persistent free radicals, reactive oxygen species generation, and oxidative potential of highway $PM_{2.5}$, ACS Earth Space Chem., 5, 1865–1875, http://dx.doi.org/10.1021/acsearthspacechem.1c00135, 2021.

Khan, F., Garg, V. K., Singh, A. K., and Kumar, T.: Role of free radicals and certain antioxidants in the management of huntington's disease: A review, J. Anal. Pharm. Res, 7, 386–392, http://dx.doi.org/10.15406/japlr.2018.07.00256, 2018.

380 Lang, D., Jiang, F., Gao, X., Yi, P., Liu, Y., Li, H., Chen, Q., Pan, B., and Xing, B.: Generation of environmentally persistent free radicals on faceted TiO_2 in an ambient environment: roles of crystalline surface structures, Environ. Sci. Nano, 9, 2521–2533, http://dx.doi.org/10.1039/D2EN00240J, 2022.

Li, H., Chen, Q., Wang, C., Wang, R., Sha, T., Yang, X., and Ainur, D.: Pollution characteristics of environmental persistent free radicals (EPFRs) and their contribution to oxidation potential in road dust in a large city in northwest China, J. Hazard.
385 Mater., 442, 130087, http://dx.doi.org/10.1016/j.jhazmat.2022.130087, 2023.

Li, Z., Zhao, H., Li, X., and Bekele, T. G.: Characteristics and sources of environmentally persistent free radicals in $PM_{2.5}$ in Dalian, Northeast China: correlation with polycyclic aromatic hydrocarbons, Environ. Sci. Pollut. Res., 29, 24612–24622, http://dx.doi.org/10.1007/s11356-021-17688-9, 2022.

Lin, M. and Yu, J. Z.: Assessment of interactions between transition metals and atmospheric organics: Ascorbic acid depletion
390 and hydroxyl radical formation in organic-metal mixtures, Environ.. Sci.. Technol., 54, 1431–1442, http://dx.doi.org/10.1021/acs.est.9b07478, 2020.

Lin, P., Hu, M., Deng, Z., Slanina, J., Han, S., Kondo, Y., Takegawa, N., Miyazaki, Y., Zhao, Y., and Sugimoto, N.: Seasonal and diurnal variations of organic carbon in $PM_{2.5}$ in Beijing and the estimation of secondary organic carbon, J. Geophys. Res. Atmos, 114, http://dx.doi.org/10.1029/2008JD010902, 2009.

395 Ma, X., Li, C., Dong, X., and Liao, H.: Empirical analysis on the effectiveness of air quality control measures during mega events: evidence from Beijing, China, J. Clean. Prod., 271, 122536, http://dx.doi.org/10.1016/j.jclepro.2020.122536, 2020.

Niu, Y., Li, X., Qi, B., and Du, R.: Variation in the concentrations of atmospheric $PM_{2.5}$ and its main chemical components in an eastern China city (Hangzhou) since the release of the Air Pollution Prevention and Control Action Plan in 2013, Air Qual Atmos Health, 15, 321–337, http://dx.doi.org/10.1007/s11869-021-01107-6, 2022.

400 Odinga, E. S., Waigi, M. G., Gudda, F. O., Wang, J., Yang, B., Hu, X., Li, S., and Gao, Y.: Occurrence, formation, environmental fate and risks of environmentally persistent free radicals in biochars, Environ Int, 134, 105172, http://dx.doi.org/10.1016/j.envint.2019.105172, 2020.

Okuda, T., Matsuura, S., Yamaguchi, D., Umemura, T., Hanada, E., Orihara, H., Tanaka, S., He, K., Ma, Y., Cheng, Y., and Liang, L.: The impact of the pollution control measures for the 2008 Beijing Olympic Games on the chemical composition of
405 aerosols, Atmospheric Environ., 45, 2789–2794, http://dx.doi.org/10.1016/j.atmosenv.2011.01.053, 2011.

Pan, B., Li, H., Lang, D., and Xing, B.: Environmentally persistent free radicals: Occurrence, formation mechanisms and implications, Environ. Pollut., 248, 320–331, http://dx.doi.org/10.1016/j.envpol.2019.02.032, 2019.

Perrone, M. G., Carbone, C., Faedo, D., Ferrero, L., Maggioni, A., Sangiorgi, G., and Bolzacchini, E.: Exhaust emissions of polycyclic aromatic hydrocarbons, n-alkanes and phenols from vehicles coming within different European classes, Atmospheric Environ., 82, 391–400, http://dx.doi.org/10.1016/j.atmosenv.2013.10.040, 2014.

Pipal, A. S., Jan, R., Bisht, D. S., Srivastava, A. K., Tiwari, S., and Taneja, A.: Day and night variability of atmospheric organic and elemental carbon during winter of 2011-12 in Agra, India, Sustain. Environ. Res., 24, 107–116, 2014.

Qian, R., Zhang, S., Peng, C., Zhang, L., Yang, F., Tian, M., Huang, R., Wang, Q., Chen, Q., Yao, X., and Chen, Y.: Characteristics and potential exposure risks of environmentally persistent free radicals in $PM_{2.5}$ in the three gorges reservoir area, Southwestern China, Chemosphere, 252, 126425, http://dx.doi.org/10.1016/j.chemosphere.2020.126425, 2020.

Qin, Y., Zhang, X., Huang, W., Qin, J., Hu, X., Cao, Y., Zhao, T., Zhang, Y., Tan, J., Zhang, Z., Wang, X., and Wang, Z.: Measurement report: Impact of emission control measures on environmental persistent free radicals and reactive oxygen species – A short-term case study in Beijing, Zenodo [Data set], http://dx.doi.org/10.5281/zenodo.10136894, 2023.

Schleicher, N., Norra, S., Chen, Y., Chai, F., and Wang, S.: Efficiency of mitigation measures to reduce particulate air pollution—a case study during the Olympic Summer Games 2008 in Beijing, China, Sci. Total Environ., 427, 146–158, http://dx.doi.org/10.1016/j.scitotenv.2012.04.004, 2012.

Sharma, S., Mandal, T., Jain, S., Saraswati, Sharma, A., and Saxena, M.: Source apportionment of $PM_{2.5}$ in Delhi, India using PMF model, Bull Environ Contam Toxicol, 97, 286–293, http://dx.doi.org/10.1007/s00128-016-1836-1, 2016.

Stevanovic, S., Gali, N. K., Salimi, F., Brown, R. A., Ning, Z., Cravigan, L., Brimblecombe, P., Bottle, S., and Ristovski, Z. D.: Diurnal profiles of particle-bound ROS of $PM_{2.5}$ in urban environment of Hong Kong and their association with $PM_{2.5}$, black carbon, ozone and PAHs, Atmospheric Environ., 219, 117023, http://dx.doi.org/10.1016/j.atmosenv.2019.117023, 2019.

Sun, Y., Wang, Z., Wild, O., Xu, W., Chen, C., Fu, P., Du, W., Zhou, L., Zhang, Q., Han, T., Wang, Q., Pan, X., Zheng, H., Li, J., Guo, X., Liu, J., and Worsnop, D. R.: "APEC Blue": Secondary aerosol reductions from emission controls in Beijing, Sci. Rep, 6, 20668, http://dx.doi.org/10.1038/srep20668, 2016.

Thevenot, P. T., Saravia, J., Jin, N., Giaimo, J. D., Chustz, R. E., Mahne, S., Kelley, M. A., Hebert, V. Y., Dellinger, B., and Dugas, T. R.: Radical-containing ultrafine particulate matter initiates epithelial-to-mesenchymal transitions in airway epithelial cells, Am. J. Respir. Cell Mol. Biol., 48, 188–197, http://dx.doi.org/10.1165/rcmb.2012-0052OC 2013.

Tong, H., Lakey, P. S. J., Arangio, A. M., Socorro, J., Shen, F., Lucas, K., Brune, W. H., Pöschl, U., and Shiraiwa, M.: Reactive oxygen species formed by secondary organic aerosols in water and surrogate lung fluid, Environ.. Sci.. Technol., 52, 11642–11651, http://dx.doi.org/10.1021/acs.est.8b03695, 2018.

Vejerano, E. P., Rao, G., Khachatryan, L., Cormier, S. A., and Lomnicki, S.: Environmentally persistent free radicals: Insights on a new class of pollutants, Environ.. Sci.. Technol., 52, 2468–2481, http://dx.doi.org/10.1021/acs.est.7b04439, 2018.

Venkatachari, P., Hopke, P. K., Grover, B. D., and Eatough, D. J.: Measurement of Particle-bound reactive oxygen species in rubidoux aerosols, J Atmos Chem 50, 49–58, http://dx.doi.org/10.1007/s10874-005-1662-z, 2005.

Verma, V., Shafer, M. M., Schauer, J. J., and Sioutas, C.: Contribution of transition metals in the reactive oxygen species activity of PM emissions from retrofitted heavy-duty vehicles, Atmospheric Environ., 44, 5165–5173, http://dx.doi.org/10.1016/j.atmosenv.2010.08.052, 2010.

Vinayak, A., Mudgal, G., and Singh, G. B.: Environment persistent free radicals: Long-lived particles, in: Free Radical Biology and Environmental Toxicity, Springer, 1–19, http://dx.doi.org/10.1007/978-3-030-83446-3, 2022.

445 Wan, Z., Sun, Y., Tsang, D. C., Hou, D., Cao, X., Zhang, S., Gao, B., and Ok, Y. S.: Sustainable remediation with an electroactive biochar system: mechanisms and perspectives, Green Chem., 22, 2688–2711, http://dx.doi.org/10.1039/D0GC00717J 2020.

Wang, L., Zhang, L., Ristovski, Z., Zheng, X., Wang, H., Li, L., Gao, J., Salimi, F., Gao, Y., and Jing, S.: Assessing the effect of reactive oxygen species and volatile organic compound profiles coming from certain types of Chinese cooking on the

450 toxicity of human bronchial epithelial cells, Environ.. Sci.. Technol., 54, 8868–8877, http://dx.doi.org/10.1021/acs.est.9b07553, 2020a.

Wang, P., Pan, B., Li, H., Huang, Y., Dong, X., Ai, F., Liu, L., Wu, M., and Xing, B.: The overlooked occurrence of environmentally persistent free radicals in an area with low-rank coal burning, Xuanwei, China, Environ.. Sci.. Technol., 52, 1054–1061, http://dx.doi.org/10.1021/acs.est.7b05453, 2018.

455 Wang, S., Song, T., Shiraiwa, M., Song, J., Ren, H., Ren, L., Wei, L., Sun, Y., Zhang, Y., and Fu, P.: Occurrence of aerosol proteinaceous matter in urban Beijing: An investigation on composition, sources, and atmospheric processes during the "APEC Blue" period, Environ.. Sci.. Technol., 53, 7380–7390, http://dx.doi.org/10.1021/acs.est.9b00726, 2019a.

Wang, Y., Hopke, P. K., Sun, L., Chalupa, D. C., and Utell, M. J.: Laboratory and field testing of an automated atmospheric particle-bound reactive oxygen species sampling-analysis system, J. Toxicol., 2011, 419476,

460 http://dx.doi.org/10.1155/2011/419476, 2011.

Wang, Y., Yao, K., Fu, X. e., Zhai, X., Jin, L., and Guo, H.: Size-resolved exposure risk and subsequent role of environmentally persistent free radicals (EPFRs) from atmospheric particles, Atmospheric Environ., 276, 119059, http://dx.doi.org/10.1016/j.atmosenv.2022.119059, 2022.

Wang, Y., Zhang, Y., Schauer, J. J., de Foy, B., Cai, T., and Zhang, Y.: Impacts of sources on $PM_{2.5}$ oxidation potential during

465 and after the Asia-Pacific Economic Cooperation Conference in Huairou, Beijing, Environ.. Sci.. Technol., 54, 2585–2594, http://dx.doi.org/10.1021/acs.est.9b05468, 2020b.

Wang, Y., Li, S., Wang, M., Sun, H., Mu, Z., Zhang, L., Li, Y., and Chen, Q.: Source apportionment of environmentally persistent free radicals (EPFRs) in $PM_{2.5}$ over Xi'an, China, Sci. Total Environ., 689, 193–202, 2019b.

Wu, S., Yang, B., Wang, X., Hong, H., and Yuan, C.: Diurnal variation of nitrated polycyclic aromatic hydrocarbons in PM_{10}

470 at a roadside site in Xiamen, China, J Environ Sci (China), 24, 1767–1776, http://dx.doi.org/10.1016/S1001-0742(11)61018-8, 2012.

Xu, Y., Yang, L., Wang, X., Zheng, M., Li, C., Zhang, A., Fu, J., Yang, Y., Qin, L., Liu, X., and Liu, G.: Risk evaluation of environmentally persistent free radicals in airborne particulate matter and influence of atmospheric factors, Ecotoxicol Environ Saf, 196, 110571, http://dx.doi.org/10.1016/j.ecoenv.2020.110571, 2020.

475 Yang, L., Liu, G., Zheng, M., Jin, R., Zhu, Q., Zhao, Y., Wu, X., and Xu, Y.: Highly elevated levels and particle-size distributions of environmentally persistent free radicals in haze-associated atmosphere, Environ.. Sci.. Technol., 51, 7936–7944, http://dx.doi.org/10.1021/acs.est.7b01929, 2017.

Yang, Y., Liu, X., Qu, Y., Wang, J., An, J., Zhang, Y., and Zhang, F.: Formation mechanism of continuous extreme haze episodes in the megacity Beijing, China, in January 2013, Atmos Res, 155, 192–203, http://dx.doi.org/10.1016/j.atmosres.2014.11.023,

480 2015.

Zhang, X., Wang, Z., Huo, P., Zhang, L., Chen, Q., and Zhang, Y.: Pollution characteristics of environmental persistent free

radicals and coexisting health risk substances in $PM_{2.5}$ in Huairou, Beijing, 41, 813–822, http://dx.doi.org/10.7524/j.issn.0254-6108.2020111901, 2022.

485 Zhang, Y., Schnelle-Kreis, J., Abbaszade, G., Zimmermann, R., Zotter, P., Shen, R., Schäfer, K., Shao, L., Prévôt, A. S. H., and Szidat, S.: Source apportionment of elemental carbon in Beijing, China: Insights from radiocarbon and organic marker measurements, Environ.. Sci.. Technol., 49, 8408–8415, http://dx.doi.org/10.1021/acs.est.5b01944, 2015.

Zhao, J., Du, W., Zhang, Y., Wang, Q., Chen, C., Xu, W., Han, T., Wang, Y., Fu, P., and Wang, Z.: Insights into aerosol chemistry during the 2015 China Victory Day parade: Results from simultaneous measurements at ground level and 260 m in Beijing, Atmos. Chem. Phys, 17, 3215–3232, http://dx.doi.org/10.5194/acp-17-3215-2017, 2017.

490 Zhao, K., Zhang, Y., Shang, J., Schauer, J. J., Huang, W., Tian, J., Yang, S., Fang, D., and Zhang, D.: Impact of Beijing's "Coal to Electricity" program on ambient $PM_{2.5}$ and the associated reactive oxygen species (ROS), J Environ Sci (China), 133, 93–106, http://dx.doi.org/10.1016/j.jes.2022.06.038, 2023.

Zheng, Y., Che, H., Zhao, T., Xia, X., Gui, K., An, L., Qi, B., Wang, H., Wang, Y., and Yu, J.: Aerosol optical properties over Beijing during the world athletics championships and victory day military parade in August and September 2015, Atmosphere, 495 7, 47, http://dx.doi.org/10.3390/atmos7030047, 2016.

Zhou, J., Zotter, P., Bruns, E. A., Stefenelli, G., Bhattu, D., Brown, S., Bertrand, A., Marchand, N., Lamkaddam, H., Slowik, J. G., Prévôt, A. S. H., Baltensperger, U., Nussbaumer, T., El-Haddad, I., and Dommen, J.: Particle-bound reactive oxygen species (PB-ROS) emissions and formation pathways in residential wood smoke under different combustion and aging conditions, Atmos. Chem. Phys., 18, 6985–7000, http://dx.doi.org/10.5194/acp-18-6985-2018, 2018.

500 Zhu, K., Jia, H., Zhao, S., Xia, T., Guo, X., Wang, T., and Zhu, L.: Formation of environmentally persistent free radicals on microplastics under light irradiation, Environ.. Sci.. Technol., 53, 8177–8186, http://dx.doi.org/10.1021/acs.est.9b01474, 2019.

Zhu, S., Zheng, X., Stevanovic, S., Wang, L., Wang, H., Gao, J., Xiang, Z., Ristovski, Z., Liu, J., Yu, M., Wang, L., and Chen, J.: Investigating particles, VOCs, ROS produced from mosquito-repellent incense emissions and implications in SOA formation and human health, Build Environ, 143, 645–651, http://dx.doi.org/10.1016/j.buildenv.2018.07.053, 2018.

505